Redox Thermodynamics of the Native and Alkaline Forms of Eukaryotic and Bacterial Class I Cytochromes *c*[†]

Gianantonio Battistuzzi,[‡] Marco Borsari,[‡] Marco Sola,*[,§] and Francesco Francia[||]

Department of Chemistry, University of Modena, Via Campi 183, 41100 Modena, Italy, Institute of Agricultural Chemistry, University of Bologna, Viale Berti Pichat 10, 40127 Bologna, Italy, and Department of Biology, University of Bologna, Viale Irnerio 42, 40126 Bologna, Italy

Received June 25, 1997; Revised Manuscript Received September 11, 1997[⊗]

ABSTRACT: The reduction potentials of beef heart cytochrome *c* and cytochromes c_2 from *Rhodopseudomonas palustris, Rhodobacter sphaeroides*, and *Rhodobacter capsulatus* were measured through direct electrochemistry at a surface-modified gold electrode as a function of temperature in nonisothermal experiments carried out at neutral and alkaline pH values. The thermodynamic parameters for protein reduction ($\Delta S°_{rc}$ and $\Delta H°_{rc}$) were determined for the native and alkaline conformers. Enthalpy and entropy terms underlying species-dependent differences in $E°$ and pH- and temperature-induced $E°$ changes for a given cytochrome were analyzed. The difference of about +0.1 V in $E°$ between cytochromes c_2 and the eukaryotic species can be separated into an enthalpic term ($-\Delta\Delta H°_{rc}/F$) of +0.130 V and an entropic term ($T\Delta\Delta S°_{rc}/F$) of −0.040 V. Hence, the higher potential of the bacterial species appears to be determined entirely by a greater enthalpic stabilization of the reduced state. Analogously, the much lower potential of the alkaline conformer(s) as compared to the native species is by far enthalpic in origin for both protein families, and is largely determined by the substitution of Met for Lys in axial heme ligation. Instead, the biphasic $E°$/temperature profile for the native cytochromes is due to a difference in reduction entropy between the conformers at low and high temperatures. Temperature-dependent ^{1}H NMR experiments suggest that the temperature-induced transition also involves a change in orientation of the axial methionine ligand with respect to the heme plane.

Knowledge of the thermodynamics of electron exchange for redox metalloproteins complements structural information in pursuing full characterization of protein function. Moreover, evaluation of the enthalpy and entropy contributions to the relative stabilization of the two redox states helps in understanding the factors that control differences in reduction potential among proteins containing the same prosthetic center or changes in redox properties of a given species due to residue mutations, pH or medium composition. The feasibility of direct protein electrochemistry at solid electrodes (*1*−*5*) has opened the way for evaluation on safe bases of redox thermodynamics of small and medium-sized redox proteins. Among class I cytochromes (cyt)[1] *c*, that from horse heart has been the most thoroughly investigated species in this respect in the past (*6*−*10*), although recently data have also been obtained for some bacterial species (*11*, *12*). The high reduction potential of this protein class (from +0.25 to +0.35 V) (*13*) turns out to be primarily the result of a sizeably negative reduction enthalpy due to the preferential stabilization of the ferroheme by ligand binding interactions, particularly the axial iron−methionine bond, and by the strongly hydrophobic environment of the heme. The small loss in entropy upon reduction of the ferri form was variably interpreted in the past, mostly in terms of subtle conformational changes of the polypeptide matrix around the heme, changes in molecular volume and solvation properties, which lead to a more structured state (*6*−*11*). Moreover, the biphasic behavior in the $E°/T$ profile for native cytochrome *c* at alkaline pH values was attributed to a conformational transition between two oxidized protein forms, possibly involving a change in protonation state (*14*, *15*).

Here, we illustrate a series of temperature-dependent cyclic voltammetry and proton NMR experiments on beef heart cytochrome *c* and on cytochromes c_2 from *Rhodopseudomonas* (*Rps.*) *palustris*, *Rhodobacter* (*Rb.*) *sphaeroides*, and *Rhodobacter* (*Rb.*) *capsulatus*. We focused on the determination of the thermodynamic parameters for the various conformers present in different pH and temperature ranges. Those for the alkaline forms are determined for the first time. Our main goals are (a) to achieve a deeper understanding of the molecular bases underlying the negative reduction entropy and the temperature-induced transition of the native form, also by reference to the recently solved NMR solution structures of both redox forms of horse heart cytochrome *c* (*16*, *17*); (b) to bring to light differences in redox thermodynamics between eukaryotic and bacterial species; and (c) to gain further insight into the equilibrium between native and alkaline conformers of this protein class.

We found that the difference in reduction potential between eukaryotic cytochromes *c* and cytochromes c_2 is for the most

[†] This work was supported by the Ministero della Pubblica Istruzione of Italy (MURST 40%)

* To whom correspondence should be addressed.
[‡] Department of Chemistry, University of Modena.
[§] Institute of Agricultural Chemistry, University of Bologna.
[||] Department of Biology, University of Bologna.

[⊗] Abstract published in *Advance ACS Abstracts,* November 1, 1997.

[1] Abbreviations: cyt, cytochrome; SCE, saturated calomel electrode; SHE, standard hydrogen electrode; N, native cytochrome *c*; N_1, low-*T* conformer of native cytochrome *c*; N_2, high-*T* conformer of native cytochrome *c*; A, alkaline conformer of cytochrome *c*.

S0006-2960(97)01535-3 CCC: $14.00

part enthalpic in origin and that the two protein families significantly differ in terms of temperature and pH ranges in which the different conformers prevail. The potential change associated to the alkaline transition turns out to be almost entirely due to an enthalpic effect for the bacterial species, while it appears to include also a certain entropic component for beef heart cyt *c*.

EXPERIMENTAL PROCEDURES

Materials. Beef heart cytochrome *c* was purchased from Sigma and further purified by cation exchange chromatography. *Rps. palustris* (DSM 127), *Rb. capsulatus* (GA), and *Rb. sphaeroides* (Ga) cytochromes c_2 were isolated and purified according to Bartsch (*18*). All chemicals were reagent grade. Nanopure water was used throughout.

Electrochemical Measurements. Cyclic voltammetry experiments were performed with a Potentiostat/Galvanostat PAR model 273A using a cell for small volume samples (V = 0.5 mL) under argon. A 2 mm diameter gold disc was used as working electrode, and a Pt sheet and a saturated calomel electrode (SCE) were used as counter and reference electrodes, respectively. The electric contact between the SCE and the working solution was obtained with a Vycor set. Potentials were calibrated against the MV^{2+}/MV^{+} couple (MV = methyl viologen). All the redox potentials reported in this paper are referred to the standard hydrogen electrode SHE. The working electrode was cleaned by first dipping it in ethanol for 10 min and then polishing it with alumina (BDH, particle size of about 0.015 μm) water slurry on cotton wool; finally the electrode was treated in an ultrasonic pool for about 10 min. To remove residual adsorbed impurities, the electrode was first set at a potential of +1 V (vs SCE) for 180 s and then subjected to 10 voltammetric cycles between +0.7 and −0.6 V at 0.1 V s^{-1}. Modification of the electrode surface was performed by dipping the polished electrode into a 1 mM solution of 4-mercaptopyridine for 30 s, then rinsing it with nanopure water (*1, 19*−*21*). Unbuffered protein solutions were freshly prepared before use and their concentration, varying from 0.1 to 0.3 mM, was checked spectrophotometrically. A 0.1 M NaCl solution was used as base electrolyte. The CV measurements were carried out several times, and the reduction potentials were found to be reproducible within ±2 mV.

Variable Temperature Electrochemistry. Experiments were performed with a nonisothermal electrochemical cell (*22, 23*). The reference electrode was kept at constant temperature (21 ± 0.1 °C), while the half-cell containing the working electrode and the Vycor junction to the reference electrode were kept under thermostatic control with a water bath, and its temperature was varied from 4 to 60 °C. With this experimental configuration, the reaction entropy ($\Delta S_{rc}°$) for reduction of ferricytochrome *c* is given by (*6, 22, 23*)

$$\Delta S_{rc}° = S_{red}° - S_{ox}° = nF(\mathrm{d}E°/\mathrm{d}T) \qquad (1)$$

Thus, $\Delta S_{rc}°$ was determined from the slope of the plot of $E°$ versus temperature. The enthalpy change ($\Delta H°_{rc}$) was obtained from the Gibbs−Helmholtz equation, namely, from the slope of the $E°/T$ versus $1/T$ plot. The nonisothermal behavior of the cell was carefully checked by determining the $\Delta H°_{rc}$ and $\Delta S°_{rc}$ values of the ferricyanide/ferrocyanide couple (*6, 9, 22, 23*).

^{1}H NMR Spectra. Proton NMR measurements were carried out on a Bruker AMX-400 spectrometer at 400.13 MHz. Typical acquisition parameters were as follows: spectral width, 40 kHz; pulse width, 6.8 μs (90° pulse); pulse delay, 0.5 s; number of scans, 512−1024. Spectra were run on 0.1−1 mM protein samples in aqueous solutions containing 10% deuterium oxide (D_2O) and were referenced to tetramethylsilane (TMS) after calibration against the water peak, set at the proper value at different temperatures (4.78 ppm from TMS at 20 °C). Water peak suppression was achieved using the super-WEFT pulse sequence (*24*). Calibration of the temperature control unit of the spectrometer was achieved by recording the spectra of ethylene glycol in water−dimethyl sulfoxide at different temperatures.

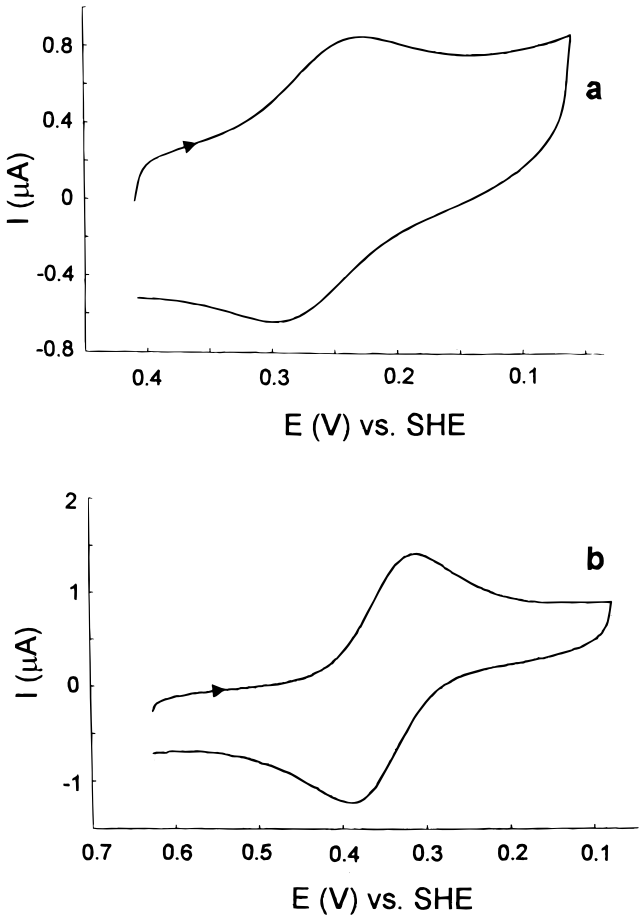

FIGURE 1: Cyclic voltammograms (third sweep) for native cytochromes *c* at a 4-mercaptopyridine surface-modified gold electrode at neutral pH: (a) beef heart cyt *c*, protein concentration, 0.09 mM; (b) *Rps. palustris* cyt c_2, protein concentration, 0.2 mM. The other cytochromes c_2 yield comparable voltammetric responses. Base electrolyte, 0.1 M NaCl; sweep rate, 0.05 V s^{-1}; T = 20 °C.

RESULTS

Redox Behavior at Room Temperature. The cyclic voltammograms for beef heart cytochrome *c* and *Rps. palustris*, *Rb. capsulatus*, and *Rb. sphaeroides* cytochromes c_2 at pH 7 and 20 °C contain a single electrochemically reversible, one-electron and diffusion-controlled voltammetric wave (wave I) (Figure 1). Voltammograms do not change appreciably after repeated cycles. For sweep rates from 0.01 to 0.5 V s^{-1} peak separations were of 0.059 ± 0.002 V, and anodic and cathodic peak currents were identical. These properties indicate that the electron transfer between the protein and the electrode is fast and that no protein adsorption and/or denaturation occurs onto the electrode surface. Thus, the $E°$ can be taken as the average of the cathodic and anodic

peak potentials. $E°$ values of +0.263, +0.362, +0.347, and +0.354 V were determined for the species from beef heart, *Rps. palustris*, *Rb. capsulatus*, and *Rb. sphaeroides*, respectively.

At pH values above 8, a new diffusion-controlled wave (wave II) is observed at negative potentials for all species, which is due to the lysine-ligated alkaline conformer(s) (*25*−*27*). This wave persists after repeated cycles, showing only a small decrease in intensity. At relatively low sweep rates (up to 0.3 V s^{-1}) the profile of this wave for beef heart cyt *c* contains only the onward cathodic peak, with no return anodic response (Figure 2a). A low-intensity anodic peak is instead detected for cytochromes c_2 (Figure 2c). Hence, reduction of the alkaline form turns out not to be chemically reversible in these conditions. This is due to the instability of the reduced alkaline conformer which transforms rapidly into the reduced native form with a proton uptake (*27*). As observed previously for yeast iso-1-cyt *c* (*27*), the intensity of the anodic peak increases with increasing sweep rate, and becomes comparable to that of the cathodic peak at 0.6 V s^{-1} for the bacterial species and at higher rates for beef heart cyt *c* (not shown). According to the theoretical analysis by Nicholson and Shain of an electrochemical process in which an irreversible chemical reaction is coupled to an electrochemically reversible electron transfer step, the rate constant of the alkaline to native conversion of the reduced form (k_2, see below) can be estimated from the sweep rate dependence of the cathodic peak potential of wave II, or of the ratio between the intensity of the anodic and cathodic peaks (*28*). Kinetic constant values of 0.98, 7.0, and 1.05 s^{-1} were obtained for *Rps. palustris* (*20*), *Rb. capsulatus*, and *Rb. sphaeroides* cyt c_2, respectively, at pH 9. The values for the bacterial species are lower than those obtained elsewhere for wild type, Ser82 and Ile82 mutants of yeast iso-1-cytochrome *c* and for horse cyt *c* (60, 75, 17, and 33 s^{-1}, respectively) (*27*).

The electron transfer process of wave II for cytochromes c_2 is electrochemically quasireversible (ΔE_p = 0.07−0.08 V). Thus the $E_{1/2}$ values of −0.056, −0.054, and −0.095 V determined for the alkaline form of *Rps. palustris*, *Rb. sphaeroides*, and *Rb. capsulatus* cyt c_2, respectively, at pH 9 and at 20 °C, can be assumed to be close to the $E°$ values. The irreversible voltammetric response obtained here at low sweep rates for beef heart cyt *c* is comparable to that observed previously for horse cyt *c* at pH 9−10 on an Au electrode functionalized with 4,4′-bipyridine (*25*, *26*) and on a glassy carbon electrode (*26*) in analogous conditions.

Upon increasing the pH in the range 8−10 the cathodic peak current of wave II increases to the detriment of wave I, while their sum remains constant and linearly dependent on $v^{1/2}$ (v = sweep rate). The current intensity of wave I titrates with pK_a values of 9.2 ± 0.1, 9.1 ± 0.1, 10.0 ± 0.1, and 8.8 ± 0.2 for bovine cyt *c* and cyt c_2 from *Rps. palustris*, *Rb. capsulatus*, and *Rb. sphaeroides*, respectively, at 20 °C (Figure 3). In the pH range 8−10 the potential of wave II is roughly independent of pH for all species. At pH values around 11, formation of a precipitate occurs for most species, which is due to partial protein denaturation.

Effect of the Temperature on the Redox Properties. The temperature dependence of the reduction potential of beef heart cyt *c* at different pH values is illustrated in Figure 4. From acidic to neutral pH, the reduction potential of the native form (wave I) shows a monotonic linear decrease with increasing temperature from 4 to 65 °C (Figure 4a). The

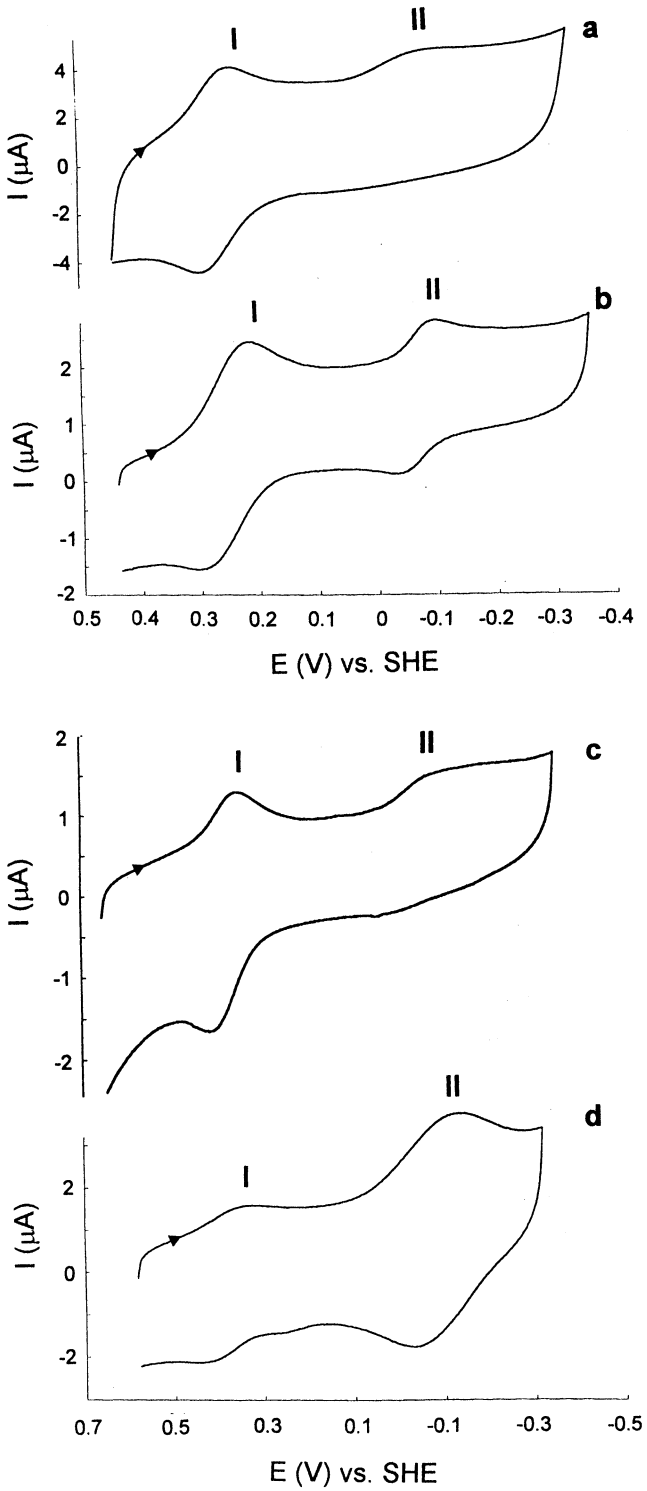

FIGURE 2: Cyclic voltammograms (third sweep) for cytochromes *c* at a 4-mercaptopyridine surface-modified gold electrode at alkaline pH: (a) beef heart cyt *c*, pH = 9.0, sweep rate, 0.05 V s^{-1}, T = 20 °C; (b) beef heart cyt *c*, pH = 9.0, sweep rate, 0.2 V s^{-1}, T = 55 °C; (c) *Rps. palustris* cyt c_2, pH = 9.0, sweep rate, 0.05 V s^{-1}, T = 20 °C; (d) *Rps. palustris* cyt c_2, pH = 9.3, sweep rate, 0.4 V s^{-1}, T = 55 °C. Base electrolyte, 0.1 M NaCl; protein concentration, 0.2 mM. I and II refer to the waves of the native and alkaline conformer, respectively.

electrochemical process is reversible throughout the temperature range investigated. At higher pH values, the $E°$ vs T plot becomes clearly biphasic with a transition point at about 50 °C (Figure 4b). The temperature of the break decreases slightly with increasing pH. This behavior was already described in detail for horse cyt *c* (*7*, *8*, *10*, *14*) and assigned to a conformational change of the ferri form (see

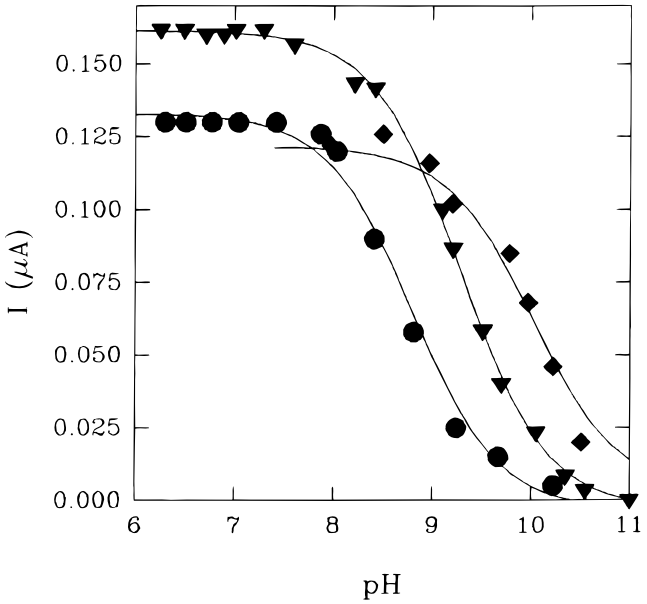

FIGURE 3: pH dependence of the cathodic peak current of wave I for cyt c_2 from *Rps. palustris* (▼), *Rb. capsulatus* (◆), and *Rb. sphaeroides* (●). Solid lines are fits to a one-proton equilibrium equation. Measurements were performed in 0.1 M NaCl. $T = 20$ °C.

below) (*14*). At pH values above 8, the irreversible reduction wave corresponding to the alkaline form (wave II) is observed. Above 40 °C wave II shows the return anodic peak also at relatively low sweep rates and the electrochemical reversibility of the process increases [peak separations, ΔE_p, were of 0.08−0.10 and 0.06−0.07 V at 40 and 55 °C, respectively (Figure 2b)]. The $E_{1/2}$ ($\cong E°$) values for this wave linearly decrease with increasing temperature (Figure 4c). Moreover, above 40 °C the currents of both anodic and cathodic peaks of wave II increase to the detriment of those of the native form (wave I), due to a *T*-induced depression of the pK_a for the alkaline transition (*29*).

Overall, the *E*°/*T* profiles indicate the presence of at least three protein forms: the low-*T* and high-*T* native conformers (N_1 and N_2, respectively) and the alkaline form (A). The A form has not yet been characterized in detail: it is known to differ from the native forms in axial heme iron ligation, due to substitution of a lysine for the methionine ligand (*30*−*36*). The $E_{1/2}$ values from −0.067 to −0.080 V determined here for alkaline beef heart cyt *c* between 40 and 65 °C (Figure 4c) differ sensibly from the midpoint potentials of −0.205 and −0.230 V obtained at 25 °C for the same form of horse heart and yeast iso-1-cytochromes *c*, respectively, on a pyrolytic graphite (edge) electrode (PGE) (*27*). This difference cannot be attributed to a temperature effect, since the $E_{1/2}$ of the latter species is expected to further decrease with increasing temperature. Due to the high sequence identity between horse and beef heart cyt *c*, this conflict is rather puzzling, although it is known that the voltammetric response for the alkaline form is remarkably affected by the pH, ionic strength, and medium composition. The rather complex mixed buffer system in which the measurements on the PGE electrode were carried out may play a role in this respect (*27*). In favor of our data, we may note that in mixed water−dimethyl sulfoxide (DMSO) solutions, [in particular, above 30% DMSO (v/v)], wave II for beef heart cyt *c* is quasireversible at 20 °C and shows an $E_{1/2}$ value of −0.036 V, which is close to the value (−0.056 V) extrapolated at the same temperature from the present experiments

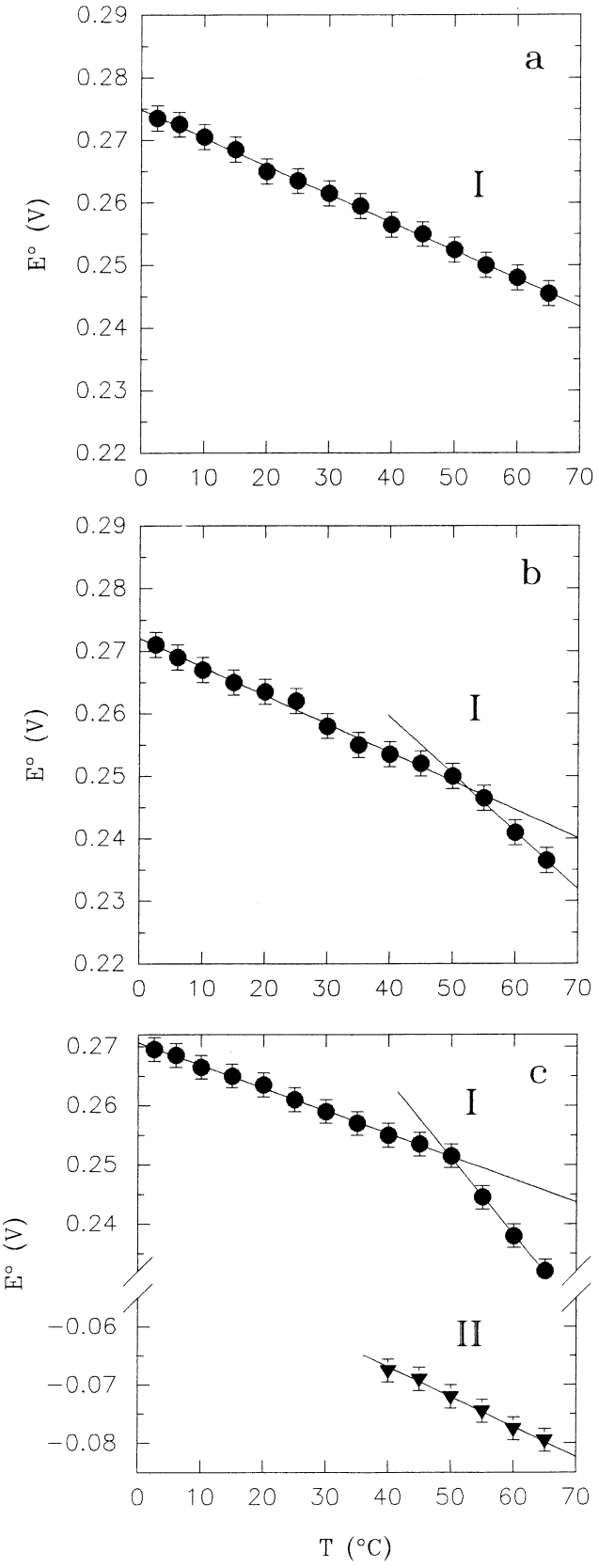

FIGURE 4: Temperature dependence of the reduction potential of beef heart cytochrome *c* at (a) pH 6.9, (b) pH 7.5, and (c) pH 8.3. Base electrolyte, 0.1 M NaCl. Solid lines are least-squares fits to the data points. I and II refer to the reduction potentials of wave I (native cyt *c*) and wave II (alkaline cyt c), respectively.

in water. Consistently, NMR shows that the organic solvent induces only a moderate conformational change in the surroundings of the heme (unpublished experiments from our laboratory).

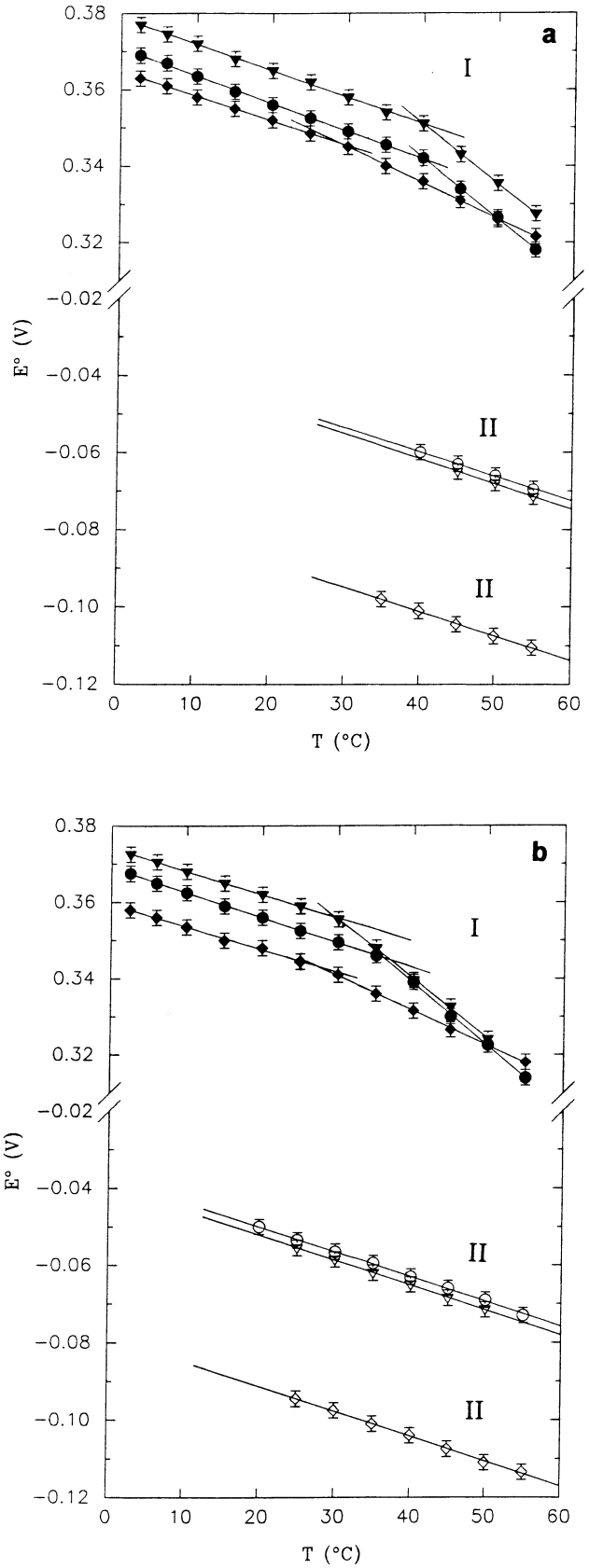

FIGURE 5: Temperature dependence of the reduction potential of cytochromes c_2 from various sources. (a) pH 6.9: *Rb. sphaeroides* (●); *Rps. palustris* (▼); *Rb. capsulatus* (◆). (b) *Rb. sphaeroides*, pH 8.6 (●); *Rps. palustris*, pH 8.5 (▼); *Rb. capsulatus*, pH 8.0 (◆). Base electrolyte, 0.1 M NaCl. Solid lines are least-squares fits to the data points. I and II refer to the reduction potentials of wave I (native cyt c_2) and wave II, (alkaline cyt c_2), respectively.

The $E°/T$ profiles for cytochromes c_2 are shown in Figure 5. The same three protein forms can be recognized, although

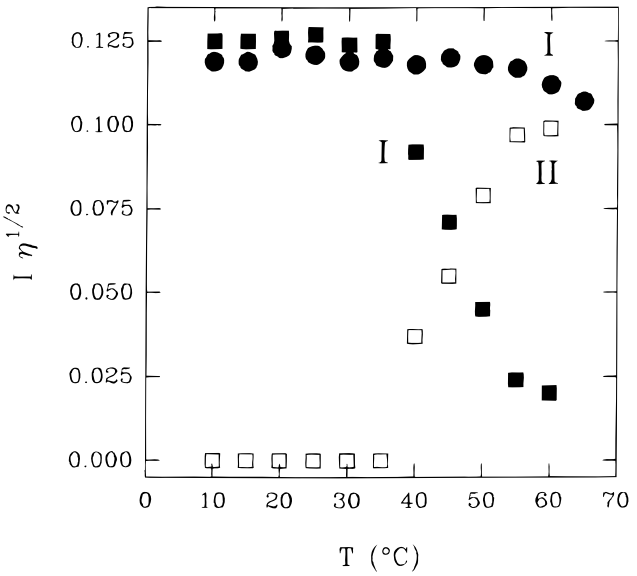

FIGURE 6: Plot of $i_d\eta^{1/2}$ (μA poise$^{1/2}$) (where i_d is the current intensity and η is the viscosity of the solution) versus temperature for beef heart cytochrome *c*, wave I, pH 7 (●), *Rps. palustris* cyt c_2, wave I, pH 7 (■), and wave II, pH 7 (□).

we may note some significant peculiarities as compared to the eukaryotic species. In particular, (i) the N_1 to N_2 transition occurs at lower pH values (as low as 6.9) with a break point at lower temperature (35−40 °C) (Figure 5a); (ii) the temperature of the transition point sensibly decreases with increasing pH (Figure 5b); (iii) the *T*-induced decrease in the pK_a for the alkaline transition is more pronounced than that for beef heart cyt *c*, as judged from the reduction wave of the alkaline form, which is observed already at pH about 7 upon increasing the temperature above 35−40 °C (Figures 5a and 6). For these species, wave II shows a good electrochemical reversibility (ΔE_p = 0.060−0.080 V) throughout the temperature range investigated.

Redox Thermodynamics. The thermodynamic parameters determined from the nonisothermal experiments described above are reported in Table 1. Published values for the native conformers of eukaryotic and bacterial species obtained from spectroelectrochemical, voltammetric and potentiometric measurements are listed in Table 2. The alkaline form has not been investigated in this respect in the past. The $\Delta S°_{rc}$ and $\Delta H°_{rc}$ values for the N_1 conformer of horse cyt *c* span a range (from −43 to −71 J mol^{-1} K^{-1} and from −38 to −44 kJ mol^{-1}, respectively) which is due, at least partially, to the different medium compositions and ionic strength in which experiments were carried out by the different authors. The redox properties of type I cytochromes *c* are indeed sensitive to the effects of protein−ion interactions (*21, 37*−*43*). Our data for this conformer of beef heart cyt *c* fall within the above ranges and, in particular, agree with the values obtained in analogous conditions (*8, 11, 14*). The reduction enthalpy and entropy for the N_2 conformer are both more negative than those for the low-*T* species and, as above, compare very well with previous values obtained by others in the same conditions (*8, 14*). The $\Delta S°_{rc}$ and $\Delta H°_{rc}$ values for the N_1 conformer of cytochromes c_2 are rather homogeneous (from −66 to −69 J mol^{-1} K^{-1} and from −52 to −55 kJ mol^{-1}, respectively), and both are more negative than the corresponding values for the eukaryotic species. Table 2 indicates that this is the case for all bacterial species investigated elsewhere but *Rhodospirillum rubrum* cyt c_2 (*6*). Regarding the thermodynamic parameters for the

Table 1: Reduction Potentials for the Native and Alkaline Forms of Class I Cytochromes *c* and $\Delta H°_{rc}$ (kJ mol^{-1}) and $\Delta S°_{rc}$ (J mol^{-1} K^{-1}) Values Determined from the Temperature Dependence of the Reduction Potential[a]

				$\Delta S°_{rc}$		$\Delta H°_{rc}$	
	pH	$E°_N$[b]	$E°_A$[b]	native	alkaline	native	alkaline
beef heart cyt *c*	6.9	+0.263		−44		−38	
	7.5	+0.262		−43		−38	
				−96		−55	
	8.3	+0.261	−0.075[c]	−37	−50	−36	−9
				−125		−65	
Rps. palustris cyt c_2	7	+0.362		−67	−62	−55	−14
				−151		−81	
	8.5	+0.359	−0.056	−60	−62	−52	−13
				−152		−80	
Rb. sphaeroides cyt c_2	7	+0.354		−69	−63	−55	−13
				−152		−81	
	9	+0.353	−0.054	−63	−61	−53	−13
				−154		−82	
Rb. capsulatus cyt c_2	7	+0.347		−66	−60	−52	−9
				−94		−61	
	9	+0.345	−0.095	−58	−61	−50	−9
				−89		−60	

[a] At 25 °C. Measurements were performed in 10 mM phosphate buffer, 0.1 M NaCl. Values in the upper and lower row for the native species refer to the low-*T* (N_1) and high-*T* (N_2) conformers, respectively. Average errors on $\Delta H°_{rc}$ and $\Delta S°_{rc}$ values are ±2 (kJ mol^{-1}) and ±6 (J mol^{-1} K^{-1}), respectively. [b] Subscripts N and A stand for native and alkaline forms, respectively. [c] $E_{1/2}$ value at 55 °C for an electrochemically quasireversible wave (ΔE_p = 0.07 V).

Table 2: Published $\Delta H°_{rc}$ (kJ mol^{-1}) and $\Delta S°_{rc}$ (J mol^{-1} K^{-1}) Values for Class I Cytochromes *c* at 25 °C

	native conformer				
	low-*T*		high-*T*		
	$\Delta S°_{rc}$	$\Delta H°_{rc}$	$\Delta S°_{rc}$	$\Delta H°_{rc}$	ref
horse cyt *c*	−53 ± 8	−40 ± 2			11[a]
	−62 ± 5	−44 ± 2			6[b]
	−50 ± 20	−44 ± 2			70[c]
	−49	−39			71[d]
	−47	−16	−193	−80	14[e]
	−44[f]	−44[f]	−137[f]	−74[f]	14[g]
	−50 ± 4	−41			10[h]
	−53	−41	−100	−56	10[j]
	−59	−42	−134	−67	10[j]
	−71				10[k]
	−53 ± 4	−41			9[l]
	−56 ± 4	−42			9[m]
	−49 ± 4	−40			7[n]
	−43 ± 6	−38	−172	−76	7[o]
	−52 ± 4	−41			8[p]
	−51 ± 5	−41	−132 ± 19	−65	8[q]
beef cyt *c*	−53 ± 8	−40 ± 2			11[a]
cyt c_2 (*R. rubrum*)	−40 ± 5	−43 ± 2			6[b]
cyt c_{551} (*P. aeruginosa*)	−68 ± 5	−47 ± 2			6[b]
cyt c_{553} (*D. vulgaris*)	−100 ± 8	−33 ± 2	−301[f]	−94[f]	11[a]
H1 (*R. viridis*)	−63	−55			72[r]
H3 (*R. viridis*)	−60	−50			72[s]

[a] Nonisothermal potentiometric titrations (Tris-HCl, I = 0.1 M, pH = 7). [b] Nonisothermal OTTLE experiments (I = 0.1 M, pH = 7). [c] Calorimetry on the oxidation of reduced cyt *c* by ferricyanide (I = 0.1 M, pH = 7). [d] Flow calorimetry on the oxidation of reduced cyt *c* by ferricyanide (0.05 M phosphate, pH = 7). [e] Nonisothermal CV experiments on a gold electrode surface modified with 6-mercaptopurine, bis(4-pyridyl)disulfide, or L-cysteine (0.1 M $NaClO_4$). [f] Determined from the plot shown in the original paper. [g] Nonisothermal CV experiments on a gold electrode surface modified with bis(4-pyridyl)disulfide (0.1 M NaCl, pH = 8.1). [h] Nonisothermal cyclic voltabsorptometry experiments on a tin-doped indium oxide optically transparent electrode (Tris-cacodylic acid buffer, I = 0.2 M, pH = 5.3). [i] Nonisothermal cyclic voltabsorptometry experiments on a tin-doped indium oxide optically transparent electrode (Tris-cacodylic acid buffer, I = 0.2 M, pH = 8). [j] Nonisothermal cyclic voltabsorptometry experiments on a tin-doped indium oxide optically transparent electrode (phosphate, I = 0.2 M, pH = 8). [k] Nonisothermal cyclic voltabsorptometry experiments on a tin-doped indium oxide optically transparent electrode (Tris-cacodylic acid buffer plus NaCl, I = 0.2 M, pH = 7). [l] Cyclic voltammetry on a tin-doped indium oxide electrode (phosphate, I = 0.2 M, pH = 7). [m] Cyclic voltammetry on a tin-doped indium oxide electrode (Tris-cacodylate, I = 0.2 M, pH = 7). [n] Cyclic voltammetry on a gold electrode modified with bis(4-pyridyl)disulfide (phosphate buffer, I = 0.1 M + 0.1 M $NaClO_4$, pH = 7). [o] Cyclic voltammetry on a gold electrode modified with bis(4-pyridyl)disulfide (phosphate buffer, I = 0.1 M + 0.1 M $NaClO_4$, pH = 8). [p] Cyclic voltammetry on a gold electrode modified with bis(4-pyridyl)disulfide (phosphate buffer, I = 0.1 M + 0.1 M NaCl, pH = 7). [q] Cyclic voltammetry on a gold electrode modified with bis(4-pyridyl)disulfide (phosphate buffer, I = 0.1 M + 0.1 M NaCl, pH = 8). [r] High potential heme H1 (cyt c_{559}) of the *Rps. viridis* reaction center. Data obtained from isothermal potentiometric experiments including correction for the temperature dependence of the potential of the reference electrode (0.01 M CHES + 0.1 M NaCl, pH = 9). [s] High-potential heme H3 (cyt c_{556}) of the *Rps. viridis* reaction center. Data obtained from isothermal potentiometric experiments including correction for the temperature dependence of the potential of the reference electrode (0.01 M CHES + 0.1 M NaCl, pH = 9).

alkaline form, we may note that for all species the $\Delta S°_{rc}$ value is very similar to that for the N_1 conformer, while the $\Delta H°_{rc}$ value is remarkably less negative.

Effect of the Temperature on the ^{1}H NMR Spectra. Proton NMR spectra were run from 15 to 60 °C at the same pH values of the above temperature dependent potential measurements. The spectral changes were analyzed mostly by reference to the well-resolved hyperfine-shifted resonances arising from the heme substituents, iron axial ligands, and residues in close proximity of the heme (*44*, *45*). These resonances are highly sensitive to changes in the heme environment, such as substitutions in axial iron ligation, acid−base and conformational equilibria, changes in the electrostatic field due to residue mutations or specific binding of anions, and interactions with solvent dipoles. The very same factors affect the relative stability of oxidized and reduced state, hence the redox potential of the protein.

At neutral and slightly acidic pH values, most of the hyperfine-shifted proton resonances of oxidized beef heart cyt *c* show a Curie law temperature behavior (not shown). No other spectral changes occur in the range of temperature investigated. This is consistent with the fact that only the low-*T* conformer of native cyt *c* is present in these conditions, as indicated by the $E°/T$ profile at these pH values (Figure 4a). At slightly alkaline pH values the chemical shift of most of the heme methyl peaks decreases linearly with increasing temperature: neither resonance broadening nor the appearance of a new pattern of methyl peaks typical of a His,Met-ligated heme is observed up to 60 °C (the peaks of the alkaline form appear at the high-temperature limit). Hence, the *T*-induced conformational transition of the oxidized native form, shown at these pH values by the $E°/T$ profile at 45−50 °C (Figure 4b), appears not to heavily affect the electronic structure of the heme. However, we noticed that the linear Curie plot of the heme methyl groups of the native species shows a slight discontinuity at a temperature of 42−45 °C (Figure 7), which does not differ much from that of the break in the $E°/T$ profile of wave I (Figure 4b,c). An analogous change in the temperature coefficient of the chemical shift of the heme 8-CH_3 and 3-CH_3 peaks can be recognized in the ^{1}H NMR spectra of the horse protein at alkaline pH (*46*). At pH about 9 the hyperfine-shifted heme methyl peaks arising from the two lysine-ligated conformers of the alkaline

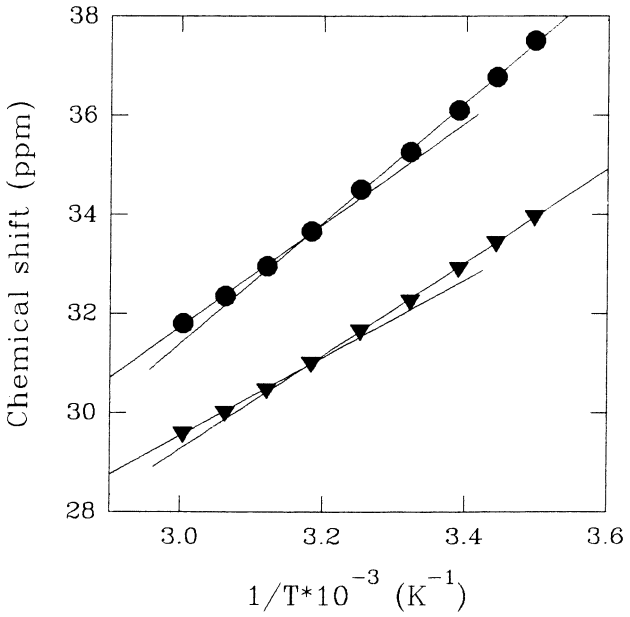

FIGURE 7: Curie plot for some ^{1}H NMR heme methyl peaks of native beef heart cytochrome *c* at pH 9: (●) 8-CH_3; (▼) 3-CH_3.

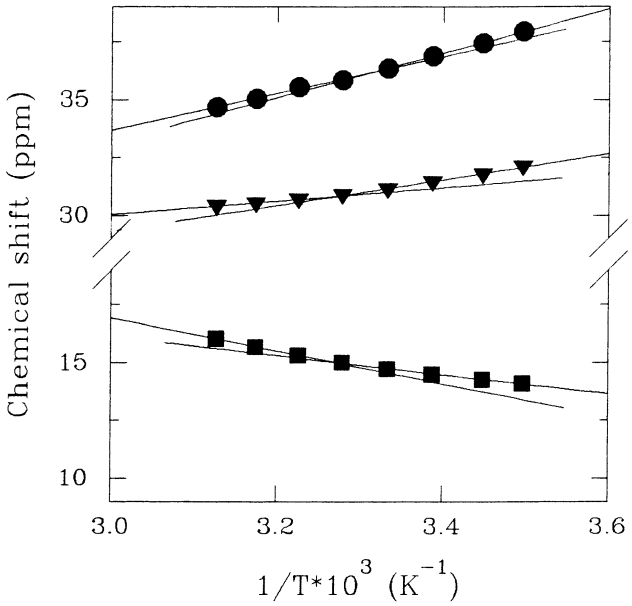

FIGURE 8: Curie plot for some ^{1}H NMR heme methyl peaks of native *Rps. palustris* cytochrome c_2 at pH 7: (●) 8-CH_3; (▼) 3-CH_3; (■) 5-CH_3.

form (A_1 and A_2) appear in slow exchange on the NMR time scale with those of the native form. These resonances are identical to those for horse ferricytochrome *c* (*46*). For both proteins, the peaks of the two alkaline species increase in intensity with increasing temperature to the detriment of those of the neutral form, with some changes in the A_1/A_2 ratio.

The *T*-induced spectral changes for the three cytochromes c_2 are comparable, and for some aspects similar to those for beef heart cyt *c*. We refer to the *Rps. palustris* species as class representative. At pH about 7 the peaks of the alkaline form appear slightly above 40 °C and increase in intensity with increasing temperature to the detriment of those of the native form, in that reproducing the temperature behavior of the current intensity of the corresponding waves in cyclic voltammetry. As above, no new hyperfine-shifted peaks attributable to the N_2 conformer are observed with increasing temperature. However, also in this case the *T* dependence of the chemical shift of the heme methyl resonances of the native species appears to be slightly biphasic. The breaks in the Curie plot and in the $E°/T$ profile of wave I occur at comparable temperatures (slightly below 40 °C) (Figures 8 and 5a). Other biphasic temperature dependencies of the chemical shift of hyperfine-shifted ^{1}H NMR heme methyl resonances of bacterial cytochromes *c* at neutral or slightly alkaline pH values were already published, but passed unnoticed (*47*, *48*). The spectral features of the hyperfine-shifted heme methyl peaks of the alkaline form are indicative of the presence of two conformers with a *T*-dependent ratio (Figure 9).

DISCUSSION

Redox Thermodynamics of the Native Form of Class I Cytochromes c. The free energy change for ferricytochrome *c* reduction is made of opposite enthalpic and entropic terms. The individual contributions to the reduction potential of this protein class are $-\Delta H°_{rc}/F = +0.43$ V, $T\Delta S°_{rc}/F = -0.17$ V and $-\Delta H°_{rc}/F = +0.53$ V, $T\Delta S°_{rc}/F = -0.20$ V for eukaryotic and bacterial cytochromes, respectively (average values obtained from the data in Tables 1 and 2). The negative enthalpy change arises primarily from the stabilization of the Fe^{2+} state due to ligand binding interactions, such as metal−ligand π back bonding at the axial methionine, the hydrophobic environment at the heme−protein interface and the small accessibility of the heme to the solvent. Protein reduction is disfavored on entropic grounds: this contribution, although smaller than the former, plays an important role in the control of the reduction potential in this protein class (*11*). In what follows we will focus on the determinants of the entropy change. The recently solved NMR solution structures of oxidized and reduced horse cytochrome *c* (*16*, *17*) offer valuable information regarding oxidation-state induced changes in protein structure and solvation properties, which can be profitably exploited for the understanding of the molecular bases of the negative reduction entropy. The partial closure of the heme crevice upon reduction is likely to be relevant in this respect (*7*−*10*). The solution structures show that the surface area of the reduced heme accessible to the solvent is smaller than that of the ferri form, as a result of differences in surface positioning of the residues which surround the exposed heme edge. In particular, Phe82, Ile81, Lys79, and Lys13 move upon protein reduction in such a way as to increase molecular packing around the heme [consistently, it has been recently calculated (*49*) that Lys79, along with Lys55, contributes much to the free energy difference between the oxidized and reduced state]. We propose that this conformational change at the heme crevice is an important structural factor underlying the small and negative entropy change associated with protein reduction. There are two main reasons. First, differences in the hydrogen bonding patterns which influence the secondary and tertiary structure of the protein in the two redox states, which do exist, may in principle affect the entropy change: however, there appears to be no net reduction-induced increase in H bonding resulting in more structured portions of the polypeptide chain, especially in the vicinity of the heme (*16*, *17*). The differences in hydrogen bonding localized at residues 60−63 in the α-helix spanning residues 60−70 and the different arrangement (α-helical or β-turn) of residues 50−55 and 70−75 may exert some minor effect. The second reason is related to consideration of the possible

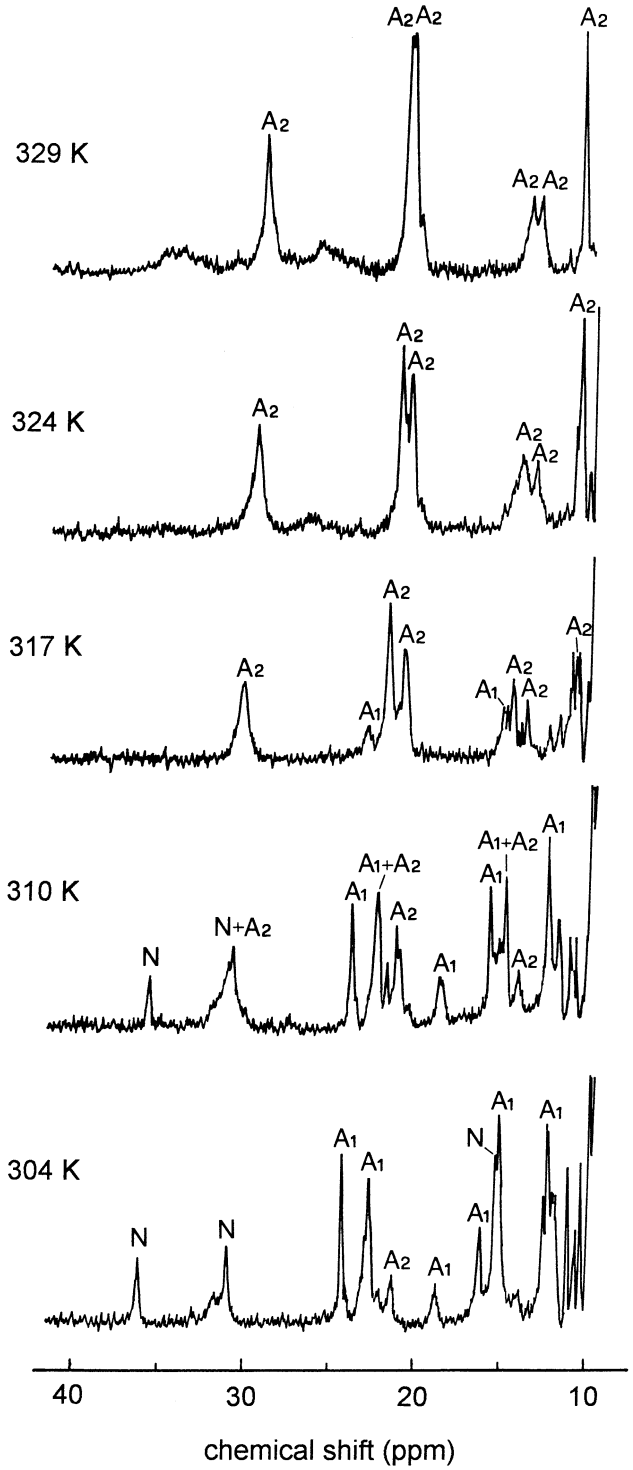

FIGURE 9: High-frequency region of the ^{1}H NMR spectrum of *Rps. palustris* cytochrome c_2 at pH 9.5 at different temperatures. Heme methyl peaks of the native form and of the two alkaline species are labeled with N, A_1, and A_2, respectively.

solvent-based contributions to $\Delta S°_{rc}$. In particular, the NMR solution structures show that, although location of structured water molecules, including the "catalytic" water molecule buried in proximity of the heme iron (*50*−*52*), is roughly similar in the two redox states, the possibility exists that the heme crevice in oxidized cyt *c* accommodates one or more additional, likely short-lived, water molecules (*17*). In this respect, it is of some interest to remind that, as shown elsewhere (*15*), the negative temperature coefficient of the reduction potential can be accounted for, also *quantitatively*, on electrostatic grounds by setting the ferriheme in a more hydrophilic environment. This in fact would allow for a greater shielding of the ferriheme from the electrostatic repulsion with the positively charged lysines clustered around the heme edge. Hence, the *T*-induced decrease in the dielectric constant of water, which determines an increase of the above electrostatic repulsion, preferentially stabilizes the oxidized over the reduced form (*15*). The NMR solution structures, however, do not confirm the closer approach of the catalytic water molecule to the iron of the ferri-heme, which instead resulted from the crystal structures (*50*−*54*), and which was considered as the responsible of the greater dielectric constant for the oxidized state. This emphasizes the role of the opening of the heme crevice in the ferri form, which facilitates solvent access, as a determinant of the temperature dependence of $E°$. However, the residence of more water molecules in the crevice of the ferriheme would contribute a positive term to the reduction entropy. Thus, it is conceivable that the oxidation-state dependence of the polypeptide packing around the heme plays a prevailing role as a determinant of the reaction entropy. Within this frame, the more negative $\Delta S°_{rc}$ values obtained for the native cytochromes with decreasing pH (Figures 4 and 5) and the opposite effect observed with increasing ionic strength (*11* and unpublished experiments from our laboratory) can be easily accounted for. In particular, the former effect should be the consequence of an increased interresidue electrostatic repulsion within the positively charged cytochrome which occurs to a greater extent in the oxidized form and determines a greater opening of the heme crevice. The latter effect is attributable to the salt-induced quenching of the above interresidue repulsion and to the decrease of the net protein charge due to specific anion binding (*42*). We may also note that the reduction entropy for the native conformers of eukaryotic and bacterial species does not differ sizably (Table 1), despite the scarce sequence identity [(from 41% to 53% among cyt c_2 and about 30% between beef heart and cyt c_2 (*13*)]. This is consistent with the reduction-induced changes being mainly localized in regions with conserved structural and sequence features such as, indeed, the heme−protein interface.

Solvent accessibility of heme propionates was proposed to be important in determining the negative reduction entropy of cytochromes *c* (*11*). This additional factor could account for the somewhat more negative $\Delta S°_{rc}$ values of the bacterial species as compared to the eukaryotic analogs. In fact, the crystal structure of *Rb. capsulatus* cyt c_2 (*55*) shows that an internal water molecule in the heme binding pocket occupies an analogous position of the catalytic water molecule in horse cyt *c*, but is much closer, and hydrogen bonded, to a carboxylate oxygen of one of the heme propionate groups. This is likely to occur also in *Rb. sphaeroides* and *Rps. palustris* cyt c_2 in which the residues involved in hydrogen bonding of the above water molecule, namely, Tyr75 and Thr94 (*Rb. capsulatus* numbering), are conserved. Following the framework outlined above, the opening of the heme crevice upon oxidation with the consequent increased solvent accessibility of heme propionates could activate this additional contribution to the entropy change in the bacterial species. Consistently, *Rsp. rubrum* cyt c_2, in which no solvent molecules are buried within the heme pocket, shows the least negative $\Delta S°_{rc}$ values (*6*) (Table 2). It is apparent, however, that solvation of the heme propionates is most likely a component, rather than the main determinant (*11*), of the entropy change in class I cytochromes *c*. Alterna-

tively, the somewhat greater entropy loss of the bacterial species could be more simply attributed to a greater increase of the polypeptide packing against the heme upon reduction as compared to the eukaryotic counterparts.

The reduction potential of cytochromes c_2 is higher than that of beef and horse cyt *c* despite an unfavorable (more negative) entropic contribution. In particular, at 25 °C, the about 0.1 V more positive $E°$ of the former species can be separated into an enthalpic term ($-\Delta\Delta H°_{rc}/F$) of +0.130 V and an entropic term ($T\Delta\Delta S°_{rc}/F$) of −0.040 V. Hence the higher potential of these bacterial species appears to be determined entirely by a greater enthalpic stabilization of the reduced state. Evaluation of the origin of the difference in $\Delta H°_{rc}$ cannot be attempted outside the framework of a suitable theoretical model, given the multiplicity of underlying electrostatic interactions involving the heme, protein charges and dipoles, and solvent dipoles.

High-T Native Conformer. The biphasic $E°/T$ profile observed at alkaline pH values for eukaryotic cytochromes *c* and in neutral or slightly acidic solution for cytochromes c_2 is still not fully understood. An electrochemical study showed that this is the result of a reversible nonequilibrium conformational transition between two states of the oxidized form which implies a fractional loss of proton on passing from the low-*T* to the high-*T* conformer (*14*). Accordingly, the biphasic $E°/T$ profile for horse cyt *c* could be reproduced through electrostatic interaction energy calculations by allowing a loss of positive charge from lysines (*15*). The decrease of the temperature of the break in the $E°/T$ profile with increasing pH is consistent with the two conformers differing in protonation state. The structural changes associated to this transition were monitored through spectral measurements. *T*-dependent circular dichroic spectra were interpreted as indicative of changes in protein conformation around the heme (*56*), while the *T*-induced decrease in intensity of the 695 nm absorption band was attributed to changes in the protein moiety that leave the Fe−S(Met80) bond unaffected (*7, 8*). The ^{1}H NMR spectra indicate that the high-*T* native conformer must not differ much from the low-*T* species in the surroundings of the heme, given that the hyperfine-shifted resonances of these two species, including those at low frequency due to the axial methionine ligand, turn out to be in fast exchange on the NMR time scale as a result of a low energy barrier for their interconversion. It is tempting to propose that the break observed in the temperature dependence of the chemical shift of the predominantly contact-shifted heme methyl resonances and that in the $E°/T$ profile, which occur at a comparable temperature for both families of cytochromes, have a common origin. This would indicate that the *T*-induced conformational change influences to some extent the electronic structure of the heme, possibly through a change in orientation of the axial methionine ligand, which is known to strongly affect the distribution of the unpaired spin density onto the heme (*57, 58*). That some *T*-induced conformational change influences the electronic structure of the heme is further demonstrated by the anomalous temperature dependence of the pseudocontact shift for the horse protein in the range 30−50 °C, a part of which must be the result of a structural change of the protein which was tentatively attributed to thermal expansion (*59, 60*).

The decrease in $E°$ which characterizes the $N_1 \rightarrow N_2$ transition turns out to be an entirely entropic effect. In fact, both reduction enthalpy and entropy of the N_2 conformer are invariably more negative than those for the N_1 species. Since the transition involves the oxidized state (*14*), it turns out that the break is due to the entropy based stabilization of the oxidized state of N_2 over that of N_1 with increasing temperature. The more negative $\Delta S°_{rc}$ values of N_2 indicate that the structural changes discussed above occur to a greater extent in this species and possibly that additional effects are operative (including that involving the proposed change in orientation of the axial methionine). The reason why the high-*T* native conformer forms at lower pH values in cytochromes c_2 as compared to the eukaryotic species is at present hardly explainable on safe bases. It may be due to a more acidic residue which triggers the conformational transition.

Overall, the thermal transition of the native form of cytochromes *c* at alkaline pH values can be depicted as a nonequilibrium transition to a conformer with a lower protonation number possessing a reduced state stabilized on enthalpic grounds but whose potential strongly decreases with increasing temperature due to a much higher entropy loss upon reduction. This is possibly the result of a greater opening of the heme crevice in the oxidized state as compared to the low-*T* conformer and of other reorganizational effects which also include a change in orientation of the axial methionine ligand.

Redox Thermodynamics of the Alkaline Form of Cytochromes c. The ^{1}H NMR spectra indicate that for class I cytochromes *c* there exist (at least) two lysine-ligated alkaline conformers (*36, 46*) (Figure 9). Since only one wave is invariably observed throughout the range of temperature investigated, these conformers turn out to possess comparable reduction potentials. The shape of the voltammetric signal sets the upper value for the difference in reduction potentials, if any, at about 0.015 V. Moreover, although the ratio of the two alkaline conformers is modulated by the temperature (Figure 9), neither discontinuities nor deviations from linearity are observed in the $E°$ vs *T* profiles (Figures 4c and 5), hence these conformers should not differ much in reduction entropy and enthalpy.

The thermodynamic data for the alkaline form of cytochromes *c* presented here, which are unprecedented, allow further insight to be gained into the determinants of the remarkably lower reduction potential of this form as compared to the native species. Besides the change in axial ligation, other factors such as changes in solvation properties are likely to play a role in this respect (*27*). The first observation is that the reduction potential of the alkaline conformer(s) does not differ much for the various species (Table 1). Hence the decrease in $E°$ on going from the native to the alkaline conformer is greater for cytochromes c_2 than for beef heart cyt *c*. Let us consider first the cyt c_2 family. The reduction entropy of the alkaline form is very similar to that of the N_1 conformer. If we consider that the reduction entropy is likely to be predominantly determined by structural changes of the polypeptide matrix responsible of heme packing, as discussed above, it turns out that such residue reorganization, hence most likely the extent of heme exposure in the two redox states, is conserved in the N_1 and A forms. Of course, it is also possible that different structural and solvent based entropy contributions in the two forms result fortuitously in very similar $\Delta S°_{rc}$ values. But this coincidence hardly occurs for three different species with low sequence identity. Thus, up to about 30−35 °C [above which the N_2 conformer is involved in the acid−base

equilibrium (Figure 5b)], the difference in reduction potential between the native and alkaline forms ($\Delta E°_{N-A}$) in cytochromes c_2 appears to be almost entirely enthalpic in origin. The $\Delta H°_{rc}$ values of the N and A forms can be interpreted in terms of relative stabilization of the heme iron in the two redox states by ligand binding interactions. The much less negative reduction enthalpy of the A form is consistent with the stronger donor properties of the ϵ-amino group of the liganding lysine, which would tend to preferentially stabilize the ferri form, as compared to the methionine sulfur of the native form, which instead stabilizes the reduced state with the contribution of metal-ligand π back bonding. The electrostatic interaction energies of solvent dipoles with the metal center would tend to stabilize the oxidized state, hence determine less negative $\Delta H°_{rc}$ values and a consequent decrease in $E°$. However, given that the exposition of the heme to the solvent should not differ much in the A and N_1 forms, as discussed above, this should be a minor effect. Likewise, differences in protein−solvent interactions in regions other than the heme crevice cannot be excluded, although at present cannot be treated with any degree of certainty, but reasonably should not remarkably affect $\Delta\Delta H°_{rc}$. Thus the change in axial ligation would appear to be the main determinant of the remarkably low $E°$ of the alkaline form in cytochromes c_2 at a relatively low temperature. Consistently, mutation of the axial methionine ligand with a lysine in the native *Thiobacillus versutus* cyt c_{550}, which is known to leave the main features of protein conformation unaffected, determines a 330 mV decrease in $E°$ (*61*), which is not too distant from the decrease in $E°$ due to the alkaline transition in the above bacterial species. At temperatures above 30 °C, where the N_2 conformer is involved in the alkaline transition, the $\Delta E°_{N-A}$ value decreases (Figure 5). This is due to the entropy contribution ($T\Delta\Delta S°_{rc}$) which becomes relevant and whose effect increases with increasing temperature.

At temperatures below 50 °C, the alkaline conformer of beef heart cyt *c* has a reduction potential lower by about 0.320 V (at pH = 8.3) than that of the N_1 form (Figure 4c). In this case, the difference in reduction entropy between the two conformers accounts for about 12% of the potential decrease ($T\Delta\Delta S°_{rc}/F = +0.040$ V, $-\Delta\Delta H°_{rc}/F = +0.280$ V). According to the framework on which we interpret the reduction entropy, the greater $\Delta S°_{rc}$ values for the alkaline form could be indicative of an increased opening of the heme crevice in the oxidized state. Thus, also the contribution of solvent dipoles to the decrease in $E°$ could be operative. As argumented above for the cytochromes c_2, the entropy contribution to the $\Delta E°_{N-A}$ value increases at temperatures (above 50 °C) in which the N_2 conformer is involved in the alkaline transition.

Equilibrium and kinetics properties of the alkaline transition of cytochromes *c* are consistent with the following minimal mechanism (*27, 32, 62*−*64*):

$$NH \overset{K_H}{\rightleftharpoons} N + H^+ \overset{k_1}{\underset{k_2}{\rightleftharpoons}} A$$

in which N and A have the usual meaning. The rapid loss of a proton by a titrating group is followed by a slow conformational transition to the alkaline form, which involves a ligand exchange equilibrium. The values of the kinetic constant k_2 estimated here from the sweep rate dependence of the anodic current of wave II, indicate that the reduced alkaline form of cytochromes c_2 converts more slowly to the reduced native form as compared to the eukaryotic species. Knowledge of the reduction potential of the native and alkaline forms and of the apparent pK_a for the alkaline transition of ferricytochromes, allows the same pK_a to be estimated for the ferro forms (*27*). Apparent pK_a values of 14.6, 16.1, 15.2, and 17.0 were obtained for bovine cyt *c* and for *Rps. palustris*, *Rb. sphaeroides*, and *Rb. capsulatus* cytochromes c_2, respectively. It is apparent that the native reduced state of the bacterial species is more stabilized with respect to the alkaline form as compared to that of the eukaryotic species. If we assume that the pK_a of the titrating group is comparable for the two classes, then the conformational transition involving ligand exchange to the alkaline reduced form turns out to be thermodynamically less favored and characterized by an higher activation barrier for the c_2 class as compared to the eukaryotic species.

The increase in current intensity of the anodic peak of wave II (corresponding to oxidation of the reduced alkaline form) with increasing temperature, which occurs for eukaryotic and bacterial species at constant sweep rate, cannot be ascribed to the increase in k_2 which should exert an opposite effect. Above 40 °C, the N_2 conformer is involved in the acid−base equilibrium with the alkaline species. Thus it appears that the activation barrier for the conversion of the reduced A form to N_2 is intrinsically higher than that to N_1.

CONCLUSIONS

Oxidation-state dependent differences in structural and solvation properties are largely the responsible of the entropy change accompanying the redox process, while the electrostatic interactions at the heme−protein interface including those with solvent dipoles, and metal−ligand electronic effects are the main factors underlying the difference in enthalpy between redox states. These two contributions modulate the reduction potential in class I cytochromes *c*. Clearly, most of oxidation-state dependent structural and electronic changes are interrelated and their individual effects are difficult to be evaluated separately. This paper shows that the enthalpy and entropy contributions to $E°$, which can be evaluated on safe bases through temperature dependent electrochemical experiments, play different roles in determining pH- or temperature-induced changes in redox properties. Hence, whichever change in $E°$ due to variation of medium conditions, residue mutation, chemical modification, or ligand binding is likely to involve both contributions which often turn out to exert opposite effects. Separation of enthalpy and entropy terms could appear a rather academic exercise in the absence of an interpretative framework which sets a correspondence between changes of structural and dynamic properties and variation of a given thermodynamic parameter (protein dynamics are expected to influence the entropic contribution to the reduction potential). We are now forced to work on qualitative bases. Establishing this correspondence is a challenge for theoretical models, which in general deal with the total electrostatic free energy (*65*−*69*), and will be a decisive step toward understanding of how redox potentials are controlled in metalloproteins.

NOTE ADDED IN PROOF

While this paper was in press, a new NMR solution structure of oxidized horse heart cytochrome *c* came out (*73*) which, at variance with that of ref 17, shows a much higher

similarity with the crystal structure of the same oxidation state (*52*) and with the solution structure of the reduced form (*16*). In particular, no evidence for the oxidation state-induced rearrangement of the side chains of surface residues at the heme edge was obtained. Moreover, recent studies of amide proton exchange rates through ^{1}H NMR show that in a number of cytochrome *c* from various sources the oxidized form possesses a greater conformation flexibility than the reduced form (*74*; I. Bertini and L. Banci, personal communication). Although it has not been established yet whether this also applies for the horse and beef heart proteins, this oxidation state-induced change would account for the fact that the reduction entropy of cytochromes *c* is negative and nearly invariant for scarely sequence-related species. Other common changes include the orientation of heme propionate-7, which is found to be disordered in the solution structure of the oxidized forms, while it is hydrogen bonded in the reduced proteins (*73*), and the presence, indicated by computational studies, of a greater number of water molecules bound in the heme cavity in the reduced state (L. Banci, personal communication). Also these additional factors would contribute a negative term to the reduction entropy.

ACKNOWLEDGMENT

Thanks are expressed to Prof. I. Bertini and Prof. L. Banci of the University of Florence, Italy, for illuminating discussion on the NMR solution structures of cytochromes *c* and for providing us some structural details prior to publication.

REFERENCES

1. Eddowes, M. J., and Hill, H. A. O. (1977) *J. Chem. Soc., Chem. Commun.* 771−772.
2. Armstrong, F. A. (1992) in *Advances in Inorganic Chemistry* (Cammack, R., Ed.) Vol. 38, pp 117−163, Academic Press, San Diego.
3. Hill, H. A. O. (1993) *NATO ASI Ser., Ser. C 385*, 133−149.
4. Bond, A. M. (1994) *Inorg. Chim. Acta 226*, 293−340.
5. Hawkridge, F. M., and Taniguchi, I. (1995) *Comments Inorg. Chem. 17*, 163−187.
6. Taniguchi, V. T., Sailasuta-Scott, N., Anson, F. C., and Gray, H. B. (1980) *Pure Appl. Chem. 52*, 2275−2281.
7. Taniguchi, I., Iseki, M., Takaki, E., Toyosawa, K., Yamaguchi, H., and Yasukouchi, K. (1984) *Bioelectrochem. Bioenerg. 13*, 373−383.
8. Taniguchi, I., Funatsu, T., Iseki, M., Yamaguchi, H., and Yasukouchi, K. (1985) *J. Electroanal. Chem. 193*, 295−302.
9. Koller, K. B., and Hawkridge, F. M. (1985) *J. Am. Chem. Soc. 107*, 7412−7417.
10. Koller, K. B., and Hawkridge, F. M. (1988) *J. Electroanal. Chem. 239*, 291−306.
11. Bertrand, P., Mbarki, O., Asso, M., Blanchard, L., Guerlesquin, F., and Tegoni, M. (1995) *Biochemistry 34*, 11071−11079.
12. Verhagen, M. F. J. M., Wolbert, R. B. G., and Hagen, W. R. (1994) *Eur. J. Biochem. 221*, 821−829.
13. Moore, G. R., and Pettigrew G. W. (1990) *Cytochromes c*, Springer-Verlag, Berlin.
14. Ikeshoji, T., Taniguchi, I., and Hawkridge, F. M. (1989) *J. Electroanal. Chem. 270*, 297−308.
15. Christen, R. P., Nomikos, S. I., and Smith, E. T. (1996) *J. Biol. Inorg. Chem. 1*, 515−522.
16. Qi, P. X., Di Stefano, D. L., and Wand, A. J. (1994) *Biochemistry 33*, 6408−6417.
17. Qi, P. X., Beckman, R. A., and Wand, A. J. (1996) *Biochemistry 35*, 12275−12286.
18. Bartsch, R. G. (1971) *Methods Enzymol. 23*, 344−363.
19. Allen, P. M., Hill, H. A. O., and Walton, N. J. (1984) *J. Electroanal. Chem. 178*, 69−86.
20. Battistuzzi G., Borsari, M., Ferretti, S., Sola, M., and Soliani, E. (1995) *Eur. J.Biochem. 232*, 206−213.
21. Battistuzzi G., Borsari, M., Dallari, D., Ferretti, S., and Sola, M. (1995) *Eur. J. Biochem. 233*, 335−339.
22. Yee, E. L., Cave, R. J., Guyer, K. L., Tyma, P. D., and Weaver, M. J. (1979) *J. Am.. Chem. Soc. 101*, 1131−1137.
23. Yee, E. L., and Weaver (1980) *Inorg. Chem. 19*, 1077−1079.
24. Inubushi, T., and Becker, E. D. (1983) *J. Magn. Reson. 51*, 128−133.
25. Haladjian, J., Pilard, R., Bianco, P., and Serre, P.-A. (1982) *Bioelectrochem. Bioenerg. 9*, 91−101.
26. Rodrigues, C. G., Farchione, F., Wedd, A. G., and Bond, A. M. (1987) *J. Electroanal. Chem. 218*, 251−264.
27. Barker, P. D., and Mauk, A. G. (1992) *J. Am. Chem. Soc. 114*, 3619−3624.
28. Nicholson, R. S., and Shain, I. (1964) *Anal. Chem. 36*, 706−723.
29. Taler, G., Schejter, A., Navon, G., Vig, I., and Margoliash E. (1995) *Biochemistry 34*, 14209−14212.
30. Hettinger, T. P., and Harbury, H. A. (1964) *Proc. Natl. Acad. Sci. U.S.A. 52*, 1469−1476.
31. Gupta, R. K., and Koenig, S. H. (1971) *Biochem. Biophys. Res. Commun. 45*, 1134−1143.
32. Davis, L. A., Schejter, A., and Hess, G. P. (1974) *J. Biol. Chem. 249*, 2624−2632.
33. Wilgus, H., and Stellwagen, E. (1974) *Proc. Natl. Acad. Sci. U.S.A. 71*, 2892−2894.
34. Smith, H. T., and Millett, F. (1980) *Biochemistry 19*, 1117−1120.
35. Gadsby, P. M. A., Peterson, J., Foote, N., Greenwood, C., and Thomson, A. J. (1987) *Biochem. J. 246*, 43−54.
36. Ferrer, J. C., Guillemette, J. G., Bogumil, R., Inglis, S. C., Smith. M., and Mauk, A. G. (1993) *J. Am. Chem. Soc. 115*, 7507−7508, and references therein.
37. Margalit, R., and Schejter, A. (1973) *Eur. J. Biochem. 32*, 492−499.
38. Margalit, R., and Schejter, A. (1973) *Eur. J. Biochem. 32*, 500−505.
39. Osheroff, N., Brautigan, D. L., and Margoliash, E. (1980) *Proc. Natl. Acad. Sci. U.S.A. 77*, 4439−4443.
40. Gopal, D., Wilson, G. S., Earl, R. A., and Cusanovich, M. A. (1988) *J. Biol. Chem. 263*, 11652−11656.
41. Arean, C. O., Moore, G. R., William, G., and Williams, R. J. P. (1988) *J. Biol. Chem. 263*, 11652−11656.
42. Battistuzzi, G., Borsari, M., Dallari, D., Lancellotti, I., and Sola, M. (1996) *Eur. J. Biochem. 241*, 208−214.
43. Battistuzzi, G., Borsari, M., and Sola, M. (1997) *Arch. Biochem. Biophys. 339*, 283−290.
44. Bertini, I., and Luchinat, C. (1996) *Coord. Chem. Rev. 150*, 1−296.
45. Bertini, I., Turano, P., and Vila, A. J. (1993) *Chem. Rev. 93*, 2833−2932.
46. Hong, X., and Dixon, D. W. (1989) *FEBS Lett. 246*, 105−108.
47. Saraiva, L. M., Denariaz, G., Liu, M.-Y., Payne, W. J., Le Gall, J., and Moura, I. (1992) *Eur. J. Biochem. 204*, 1131−1139.
48. Banci, L., Bertini, I., Cambria, M. T., Capozzi, F., and Dikiy, A. (1994) *Eur. J. Biochem. 219*, 663−669.
49. Muegge, I., Qi, P. X., Wand, A. J., Chu, Z. T., and Warshel, A. (1997) *J. Phys. Chem. B 101*, 825−836.
50. Takano, T., and Dickerson, R. E. (1981) *J. Mol. Biol. 153*, 79−94.
51. Takano, T., and Dickerson, R. E. (1981) *J. Mol. Biol. 153*, 95−115.
52. Bushnell, G. W., Louie, G. V., and Brayer, G. D. (1990) *J. Mol. Biol. 214*, 585−595.
53. Louie, G. V., and Brayer, G. D. (1990) *J. Mol. Biol. 214*, 527−555.
54. Berghuis, A. M., and Brayer, G. D. (1992) *J. Mol. Biol. 223*, 959−976.
55. Benning, M. M., Wesenberg, G., Caffrey, M. S., Bartsch, R. G., Meyer, T. E., Cusanovich, M. A., Rayment, I., and Holden, H. M. (1991) *J. Mol. Biol. 220*, 673−685.
56. Yuan, X., Hawkridge, F. M., and Chlebowski, J. F. (1993) *J. Electroanal. Chem. 350*, 29−42.
57. Senn, H., Keller, R. M., and Wüthrich, K. (1980) *Biochem. Biophys. Res. Commun. 92*, 1362−1369.

58. Satterlee, J. D. (1986) *Annu. Rep. NMR Spectrosc. 17*, 79−178.
59. Turner, D. L., and Williams, R. J. P. (1993) *Eur. J. Biochem. 211*, 555−562.
60. Santos, H., and Turner, D. L. (1992) *Eur. J. Biochem. 206*, 721−728.
61. Ubbink, M., Campos, A. P., Teixeira, M., Hunt, N. I., Hill, H. A. O., and Canters, G. W. (1994) *Biochemistry 33*, 10051−10059.
62. Lambeth, D. O., Campbell, K. L., Zand, R., and Palmer, G. (1973) *J. Biol. Chem. 248*, 8130−8136.
63. Kihara, H., Saigo, S., Nakatani, H., Hiromi, K., Ikeda-Saito, M., and Iizuka, T. (1976) *Biochim. Biophys. Acta 430*, 225−243.
64. Nall, B. T., Zuniga, E. H., White, T. B., Wood, L. C., and Ramdas, L. (1989) *Biochemistry 28*, 9834−9839.
65. Warshel, A., Papazyan, A., and Muegge, I. (1997) *J. Biol. Inorg. Chem. 2*, 143−152.
66. Zhou, H.-X. (1997) *J. Biol. Inorg. Chem. 2*, 109−113.
67. Bertini, I., Gori-Savellini, G., and Luchinat, C. (1997) *J. Biol. Inorg. Chem. 2*, 114−118.
68. Mauk, A. G., and Moore, G. R. (1997) *J. Biol. Inorg. Chem. 2*, 199−125.
69. Gunner, M. R., Alexov, E., Torres, E., and Lipovaca, S. (1997)- *J. Biol. Inorg.Chem. 2*, 126−134.
70. George, P., Eaton, W. A., and Trachman, M. (1968) *Fed. Proc., Fed. Am. Soc. Exp. Biol. 27*, 526.
71. Watt, G. D., and Sturtevant, J. M. (1969) *Biochemistry 8*, 4567−4571.
72. Gao, J. L., Shopes, R. J., and Wraight, C. A. (1990) *Biochim. Biophys. Acta 1015*, 96−108.
73. Banci, L., Bertini, I., Gray, H. B., Luchinat, C., Reddig, T., Rosato, A., and Turano, P. (1997) *Biochemistry 36*, 9867−9877.
74. Banci, L., Bertini, I., Bren, K. L., Gray, H. B., Sompornpisut, P., and Turano, P. (1997) *Biochemistry 36*, 8992−9001.

BI971535G